25th ABCM International Congress of Mechanical Engineering
October 20-25, 2019, Uberlândia, MG, Brazil

CHASSIS TORSIONAL RIGIDITY: VALIDATION OF FEA DATA BY EXPERIMENTAL TEST

Luís Fernando Marzola da Cunha
Matheus Lisboa Cardoch Valdes
Rhander Viana
Danilo dos Santos Oliveira
Faculty of Gama - University of Brasília
fernandoluismc@gmail.com, matheuscardoch@gmail.com,rhanderviana@gmail.com,unbdanilo@gmail.com
Luiz Eduardo Rodrigues Vieira
Universidade Federal de Uberlândia, Campus Santa Mônica, CEP: 38400-097, Uberlândia-MG
luizeduardoodrigues@gmail.com

Abstract. *This paper exposes how the torsional stiffness of a formula SAE student's (FSAE) frame can be evaluated by bench testing and comparing the results from two different models of testing. The team FGR UnB provides his chassis for the test with two different types of clamping to observe its consequences. The final results did not allowed to validate the computational model, however, permits to observe important factors along the bench testing and corroborate some patterns of the results. These modelling setups were analysed and tested on a same tubular chassis: the first aims to be as similar as possible to the real suspension anchor points and the second is simplest than first, and is analogous to models used since 1990's decade, to obtain a reasonable chassis' stiffness results that can be useful to some situations.*

Keywords: *Torsional Rigidity, Formula SAE Chassis, Model*

1. INTRODUCTION

The Formula SAE competitions challenge teams of university's undergraduate and graduate students to conceive, design, fabricate, develop and compete with small formula style vehicles (FSAE, 2018). In this context, the University of Brasilia (UnB) has the electrical car team FGR that develops its own project. The frame of an automobile has the purpose of connecting the front and rear suspensions while providing attachments points for the different systems of the car (III and Salinas, 1996).

The frame's torsional rigidity can be described, in an easy way to understand, as the difficulty imposed by the configuration and material rigidity of the frame to the torsional movement caused by cornering and it's effects to the chassis, and it's simplified mechanical perspective can be seen at Fig.(1). Another perspective to understand the torsional rigidity may be the physical analysis, by its measurement unit that is $\frac{N.m}{degree}$.Along well developed and integrated teams' projects, others attached components are used to increase the torsional rigidity, as the engine for example (William Milliken and Douglas Milliken, 1995).

The magnitude of a frame's stiffness is a characteristic related to the vehicle and circuit purpose. As the suspension's project team usually assume the frame as a stiffness body, consequently the frame's project team must set as target the highest rigidity possible (Tanawat Limwathanagura, 2012). However, like almost everything in engineering, it can not be stated that this is a desired characteristic for any and all situations, for a formula student structure team usually it is a good setting goal in the majority.

Since the torsional rigidity has an influence on the first of the principal objectives setting by William Milliken and Douglas Milliken (1995), that is the maintenance of cornering balance (neutral steer) under maximum lateral conditions, this feature deserves due attention along with designing, constructing and validating the vehicle.

The results can be very different depending on the method used to determine the torsional rigidity. The comparison between a traditional model and an alternative and simpler model is made with aid of an experimental apparatus built for this purpose.

The physical integrity of the chassis can be preserved during the tests. Usually, the loads applied on these torsional rigidity tests require slightly. However, it is important to verify during the simulations if the stresses and strain continue in the elastic regime to avoid compromise its integrity.

Finally, it is important also to the bench tests and its complements to be as rigidity as possible (it has to be verified

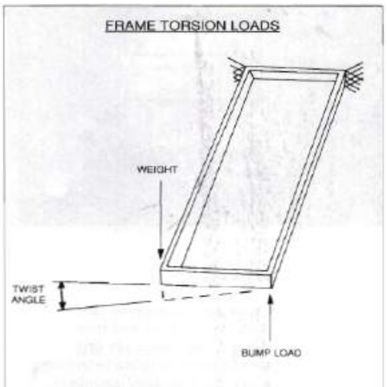

Figure 1: Mechanical Principle Scheme of Torsion Loads - Adams (1993)

Figure 2: Simple Test Adams (1993)

during its project), due to the possibility of its deformation during the test and consequently the appearance of residuals in results.

2. METHODOLOGY

Once there is the chassis projected and constructed, is important to verify the math models and determine exactly what characteristics the structure has achieve in terms of torsional rigidity. The torsional rigidity can be calculated by the ratio between an applied torque and its resultant angular deflection of known points at the frame (Riley and George (2002a)).

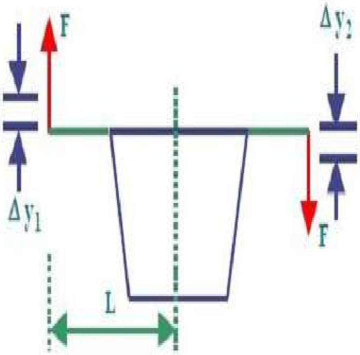

Figure 3: Front Suspension Test Loads [0]

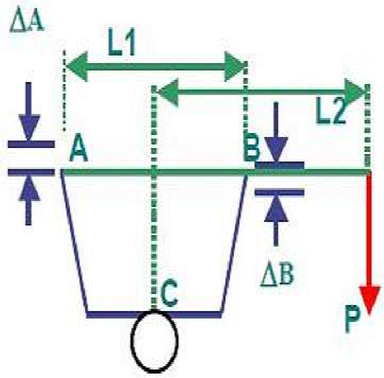

Figure 4: Front Suspension Test Loads [0]

The equations (1), (2) and (3) allows to calculate the torsional rigidity K_T through two symmetrical points of the chassis. Usually as result is presented the torsional rigidity along an upper and lower guidelines along the frame. It is important to notice that each singular point of chassis has it own torsional rigidity, even if the most usual is to present the result from average of left and right deflections.

$$K_T = \frac{T}{\theta} \tag{1}$$

$$\theta = tan^{-1}\Big(\frac{\Delta_A + \Delta_B}{L_1}\Big) \tag{2}$$

$$K_T = \frac{P(L_1 + 2L_2)}{tan^{-1}\Big(\frac{\Delta_A+\Delta_B}{L_1}\Big)} = \frac{FL}{tan^{-1}\Big(\frac{\Delta y_1+\Delta y_2}{2L}\Big)} \tag{3}$$

The calculation of torsional rigidity is the same for any kind of bench test setup, since all that is necessary is the vertical deflection and distance of this point to the axis of reference to the applied torque, which coincide with frame's central plane (other representation can be found at Barari *et al.* (2011)).

In order to facilitate the points of interest's identification, the Fig.(5) present the adopted nomenclature.

[0]Figures 3 and 4 - Riley and George (2002a)

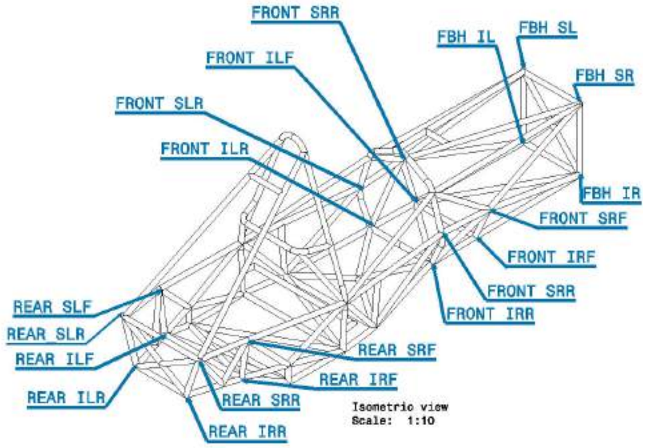

Figure 5: Identification of points/nodes - Author

The model should achieve the reality of cornering. Thus proposed models cover the maximum real transfer load from suspension to the frame at the first model and the most used method among most types of frames at the second model of this article, which has the primary disadvantage of create load paths that do not represent the same manner as on the tracker (Riley and George (2002a)).

The models should follow some rules or advises that are applied also to the basic concept of designing a space frames, it is desirable to have a triangulated frame to increase rigidity [Adams (1993)] and also the loads be applied properly on nodes. Therefore, if these two statements are respected, the frame's tubes will be subjected just by traction and compression while avoiding it to working on bending, because of that it is important to remember this also while modelling the tests.

It was decided to evaluate two methodologies through, the first one is based on the traditional torsional stiffness test where the rear suspension points are clamped and a torque is applied on the front suspensions points (Riley and George, 2002b), the second model is simplest than model 1 and is currently used since 90's decade as shown in Fig(2). The model two of this paper consists of clamping the bottom two symmetrical mounting points of the chassis, at front and rear suspension, instead of the all suspension mounting points.

During the experiments on bench test, the frame is mounted as the respective boundary conditions adopted and a dial indicator (Mitutoyo 2046s) is used to check the displacement of each point. The methodology should respect and notice some principles related to scientific methods as *accuracy, resolution, hysteresis, precision, calibration, gain, offset and noise* to avoid bad data and consequently erroneous analysing accordingly William Milliken and Douglas Milliken (1995). For all points were made 5 measurements, and the experimental process error was calculated with T Student's bicaudal distribution (2,571) with 95% of confidence level.

2.1 Experimental test

The torsion rig in Fig. (6) uses "I" section steel beams, it is composed by two basis, the rear basis beams are connected through welding and the front basis has a pivot in the center that allows the application of torque. The load is applied using weights. To attach the frame to the rig, a connection element, in red Fig. (7), was designed with the same geometry of the A-arms suspension. The measurement of deflection is made with dial indicators. There are several types of torsion rigs and measurement styles for the same purpose, they diverge in terms of results, construction demand time and costs for the test, for instance, the use of 3D motion capture techniques (Featherston *et al.*, 2005).

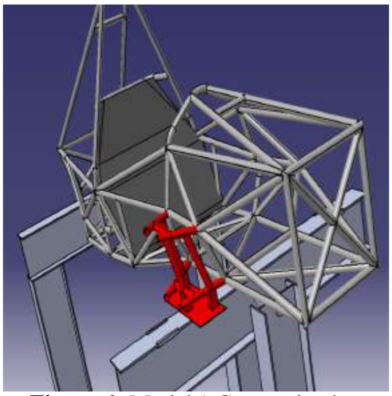

Figure 6: Model 1:Connection between the chassis and the apparatus

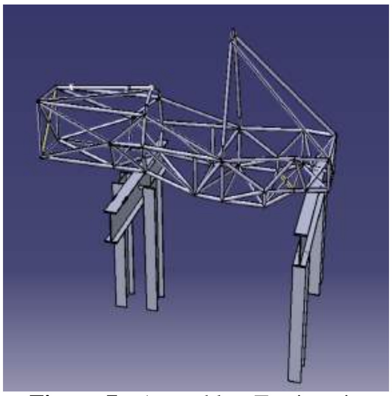

Figure 7: Assembly: Torsion rig and Chassis - Model 2

2.1.1 Model 1

Having considered the importance of mounting the points to receive the forces on triangle's nodes, it is also reasonable to look at the model and perceive that applying the forces at suspension's points is the best way to simulate the reality of cornering, which is the event that provides the torsion on chassis.

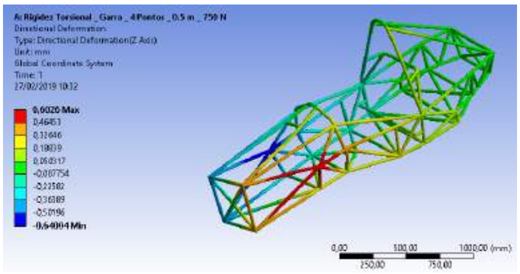

Figure 8: Model 1 View - Total Deformation Z - Author

Figure 9: Model 1 View - Experimental

The model 1 consists on fix the anchor points SRR, IRR, SRF, IRF, SLR, ILR, SLF, ILF from suspension's rear and the equivalent points from suspension's front using a specific connection element (Fig. 7) to each part of suspension.

2.1.2 Model 2

In order to have a simplest experimentation and aiming reasonable results, depending on the situation, the model 2 represented at Figs. (7) and (11) may be the best option.

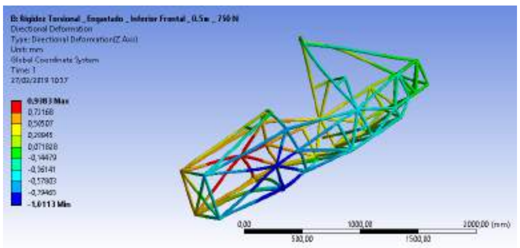

Figure 10: Model 1 View - Total Deformation Z - Author

Figure 11: Model 2 View - Experimental

The model 2 consist on fix the points IRR and ILR from suspension's rear and IRF, ILF from suspension's front by clamps as can be observed at Fig. (11).

2.2 Numerical model

In order to mesh the domain, ANSYS 18 Workbench was used, the properties of the mesh and material are found in the Tab. 1. The simulation was performed with two different elements. The first one is the BEAM 189, a 3-node beam element that is based on the Timoshenko beam theory , the second element is the SOLID 187, a 3D 10-node element that is able to represent irregular geometries (Tadeusz Storlaski, 2018), such as the tubes' notch.

Table 1: Mesh and material data

Type of element	SOLID 187	BEAM 189
Number of nodes	1496606	259347
Number of elements	592385	87326
Material density	7850 kg/m^3	same
Young's Modulus	2E11 Pa	same
Poisson's Ration	0.3	same
Behaviour	Isotropic	same

The purpose of present two methodologies in this paper is to qualifying and quantifying the results achieved from a methodology considered completed and other simpler, the boundary conditions are represented at Fig. (12) and (13) respectively.

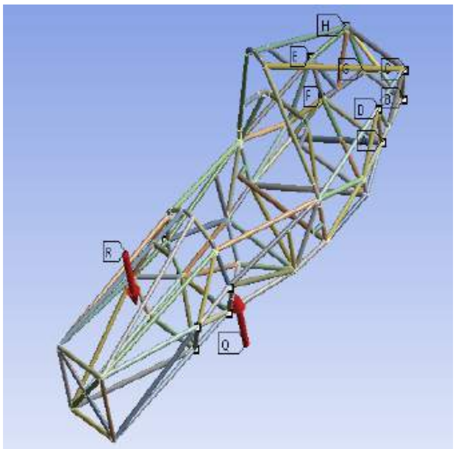

Figure 12: Model 1 View - Isometric - Author

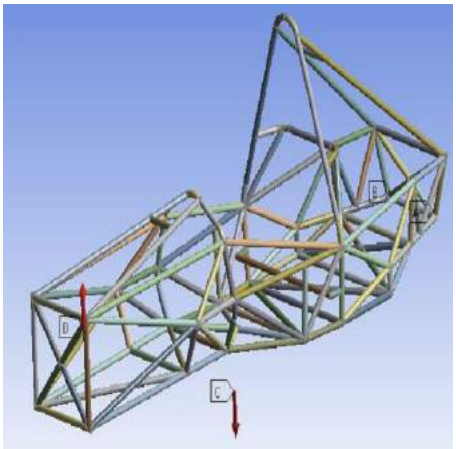

Figure 13: Model 2 View - Isometric - Author

The applied forces have the magnitude of 760 N and their distance from the chassis' center line is 500 mm. The spread distance is measured from the point of interest to the symmetrical plane which coincides chassis' centre and the torque results from the twisted force and its distance from the same plane.

To model 1 were applied two different boundary condition's setup, the first allows the displacement long Z and rotation along X of rear suspension's points SLF, SLR, ILF, ILR, SRF, SRR, IRF and IRR, and the second boundary condition setup allow only displacement along Z. For both computational setup were applied remote force at frontal suspension's points SLF, SLR, ILF, ILR, SRF, SRR, IRF, and IRR, at 0.5m distant from center.

The boundary conditions applied at computational simulation to model 2 were fixed support at the mounting points of rear suspension IRR and ILR and a remote force acting on front suspension's points IRF and ILF, at 0.5m distant from center.

3. RESULTS AND DISCUSSIONS

The experimental results from bench testing are presented at Tab.(2) and allow to observe that in general the model 2 has less error than 1, and some points as ILF, ILR SIS2 tend to have a bigger error. The error associated at ILR is null because it has no displacement, since is fixed at the bench test and has no displacement.

The experimental error can arise because of some factors, accordingly to the methodology executed, they are :

- Slipping of the dial indicator on its pickup point
- Bending in the rear connecting elements
- slightly angled between vertical direction and real setup of the dial indicator

Table 2: Experimental Errors (T-Student - Bicaudal - 95% Confidence Level)

	Experimental Error (%)											
	Frontal				Side Impact				Rear			
	SLF	SLR	ILF	ILR	SIS1	SIS2	SII1	SII2	SLF	SLR	ILR	ILR
Model 1	6,36	1,52	9,88	3,65	4,68	3,60	7,57	3,37	6,54	6,99	5,03	10,38
Model 2	3,59	8,31	13,32	7,78	1,51	17,81	1,92	1,66	1,89	7,92	4,67	0

The Figure (14) present the displacement of each point along the chassis, beginning from point 1 on left to point 6 that represents respectively for upper line the points SLF (Frontal), SRR(Frontal), SIS1 (Side Impact), SIS2 (Side Impact), SLF (Rear), SRR(Rear) and for bottom line ILF (Frontal), IRR(Frontal), SII1 (Side Impact), SII2 (Side Impact), ILF (Rear), IRR(Rear). The dotted line represents the Model 1 results and the continued line the results of Model 2.

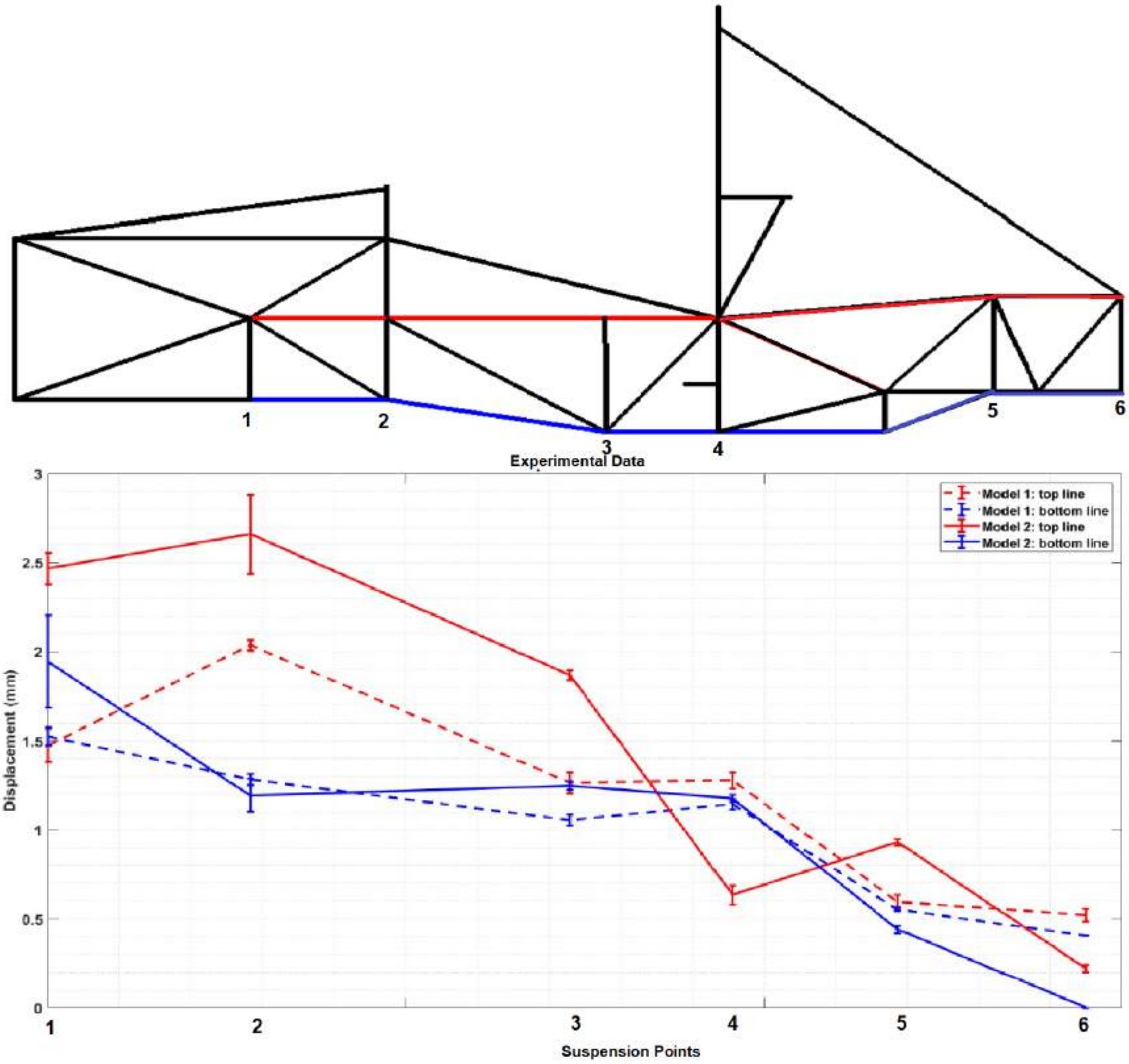

Figure 14: Displacement Models 1 and 2

As expected, model 1 has definitely bigger torsional rigidity, since the displacement along chassis due to torsional loads are smaller. The model 1 does not subject the frame to loads as the real track does with the integration of suspension on all chassis' mounting points (Riley and George (2002a)). For this reason, this work aimed to compare the results from both models.

Therefore, the Figure (15) present the comparative between experimental results of model 2 and its computational results. The key factor to corroborate the computational data with the experimental is to reproduce the correct boundary conditions. Therefore some different kind of boundary conditions were tested, since fixed support at rear mounting points until more specifics that are shown at Fig.(15).

The Continued line represents the computational results from model 2 with suspension's rear points SLF, SLR, ILF, ILR, SRF, SRR, IRF, IRR only with displacement along Z free.

The dotted line with dot at the points of interest represents the computational results from model 2 with suspension's rear points SLF, SLR, ILF, ILR, SRF, SRR, IRF, IRR only with displacement along Z free and rotation around X free.

The experimental results are shown whit simple dotted line, and for all three the red represent upper chassis's guideline and blue, bottom.

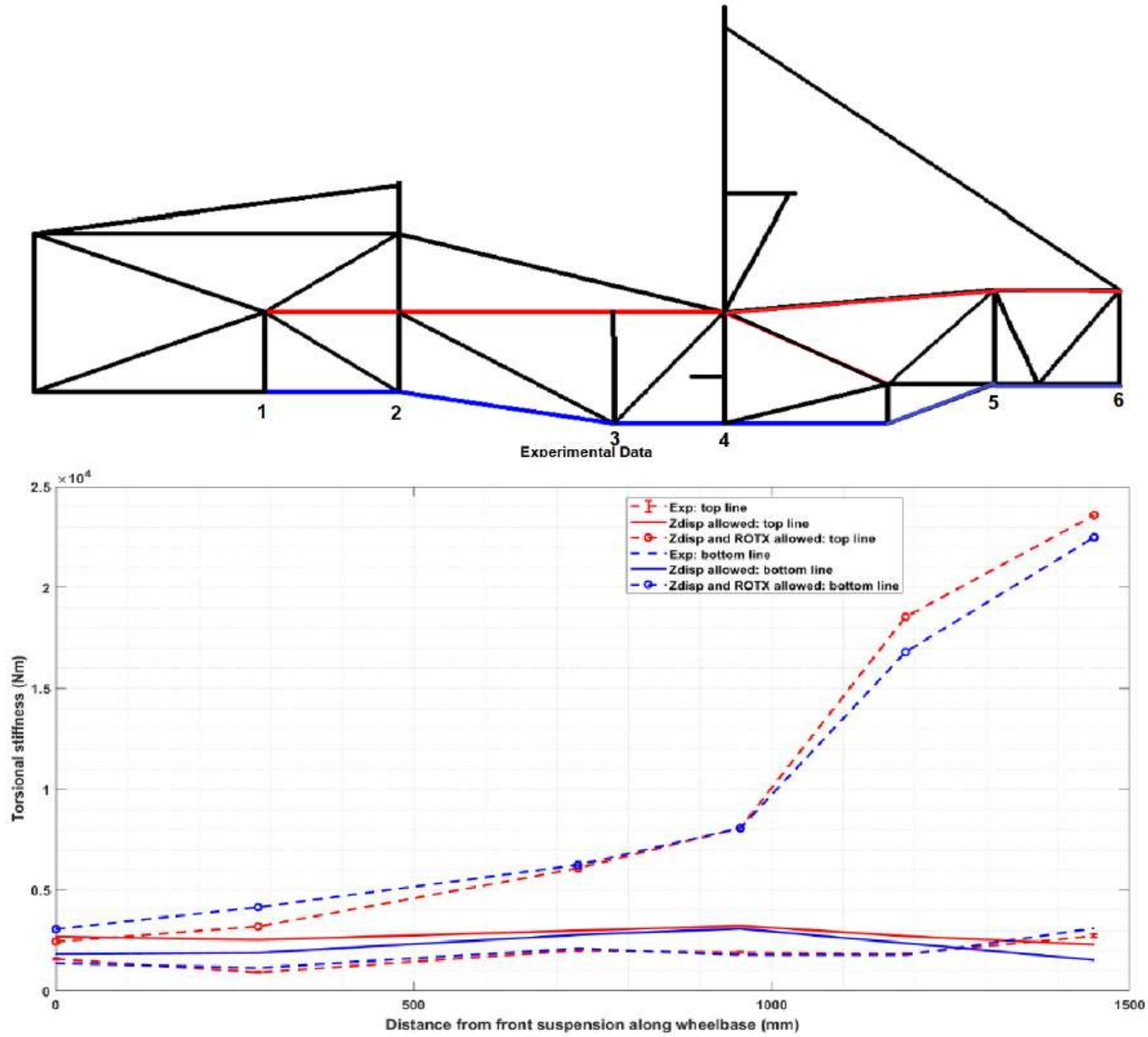

Figure 15: Displacement Models 1 and 2

Thus, from Figure (15) is possible to observe that the rotation around X increases the divergence between computational and experimental data, actually is very clear how it occurs right on the points 5 and 6 that are coincident to the rear suspension mounting points.

The Table (3) present the comparison for model 1 between experimental and computational results. The magnitude of found errors does not allow to validate the computational data, however is possible to observe that the torsional rigidity path along all the frame is similar for both, experimental and computational (Z Free) results.

Table 3: Torsional Rigidity $\frac{Nm}{degree}$ - Experimental x Computational Data

	Guideline	1	2	3	4	5	6
Experimental	Upper	1414,23	1183,83	2155,18	1828,72	1824,25	3177,7
	Bottom	1631	959	2049	1971	1896	2807
Coputational Z free	Upper	2706,23 (39,73%)	2550,84 (62,4%)	3000,23 (34,3%)	3236,51 (39,10%)	2734,73 (30,66%)	2311,38 (21,44%)
	Bottom	1842,61 (30,29%)	1899,67 (60,46%)	2797,8164 (29,81%)	3093,99 (69,18%)	2380,47 (30,48%)	1536,67 (51,64%)

4. CONCLUSION

The comparison of results did not achieve deviation parameters that allows to validate the boundary conditions applied to the computational simulation's results. Differences between 21,44% and 69,18% from torsional rigidity calculated experimentally to computational can be observed at Tab. (3). This emphasises the importance of validating the simulation methods, which means that with only a simulation, without a previous model validation, is not enough to give information about the real physical behaviour.

However, this work allows to make the comparison between model 1 and 2, and confirm that the model 2 can be used for estimate a previous torsional rigidity, without any problems related to security since it underestimate the torsional rigidity of the chassis working on all complete mounting points.

Related to the experiments, it is possible to conclude that is very important to give due attention to the positioning of dial indicator and be careful to avoid sliding. The properly measurements acquisition to calculate the error will give results with more credibility, so it should not be ignored.

Finally, in respect to the validation and corroboration of experimental and FEA data could not be achieved, however it is possible to observe that the boundary conditions that is more close was the points SLF, SLR, ILF, ILR, SRF, SRR, IRF, and IRR from rear suspension allowed just to displace along Z.

5. REFERENCES

Adams, H., 1993. *Chassis engineering : chassis design building tuning for high performance handling*. Berkley Publishing Group, 375 Hudson Street New York, New York 10014, first edition edition.

Barari, A., Tebby, S. and Esmailzadeh, E., 2011. "Methods to determine torsion stiffness in an automotive chassis". *Computer-Aided Design and Applications*, Vol. 1, pp. 67–75. doi:10.3722/cadaps.2011.PACE.67-75.

Featherston, C., Holford, K., Holt, C., Manning, D. and Claisse, A., 2005. *Measuring the Torsional Stiffness of a Space Frame Chassis Using 3D Motion Capture Techniques*, Vol. 3-4, pp. 423–428. doi:10.4028/www.scientific.net/AMM.3-4.423.

FSAE, 2018. "Rules 2019".

III, E.F.G. and Salinas, A.R., 1996. "Introduction to formula sae suspension and frame design". *SAE*.

Riley, W.B. and George, A.R., 2002a. "Design, analysis and testing of a formula sae car chassis". In *Proceedings of the 2002 SAE Motorsports Engineering Conference and Exhibition (P-382)*. Indianapolis, Indiana.

Riley, W.B. and George, A.R., 2002b. "Design, analysis and testing of a formula sae car chassis". *SAE TECHNICAL PAPER SERIES*, p. 382.

Tadeusz Storlaski, Yuji Nakasone, S.Y., 2018. *Engineering Analysis with ANSYS Software*. Elsevier, The Boulevard, Langford Lane, Kidlington, Oxford OX5 1GB, United Kingdom, second edition edition.

Tanawat Limwathanagura, Chartree Sithananun, T.L.T.S., 2012. "The frame analysis and testing for student formula". *International Journal of Mechanical and Mechatronics Engineering*, Vol. 6, No. 5, pp. 998–1002.

William Milliken, W. and Douglas Milliken, D., 1995. *Race Car Vehicle Dynamics*. Society of Automotive Engineers, Inc, 400 CommonwealthDrive Warrendale, PA 15096-0001 USA, first edition edition.